International Journal of Pharmaceutics 416 (2011) 195–201

Contents lists available at ScienceDirect

International Journal of Pharmaceutics

journal homepage: www.elsevier.com/locate/ijpharm

Preparation and *in vitro* evaluation of silk fibroin microspheres produced by a novel ultra-fine particle processing system

Xinguo Wen[a,b], Xinsheng Peng[a,c], Han Fu[a], Yixuan Dong[a], Ke Han[a], Jianfen Su[a], Zhouhua Wang[a], Rongchang Wang[a], Xin Pan[a,b], Lin Huang[a], Chuanbin Wu[a,b,*]

[a] School of Pharmaceutical Sciences, Sun Yat-sen University, Guangzhou, PR China
[b] Research and Development Center of Pharmaceutical Engineering, Sun Yat-sen University, Guangzhou, PR China
[c] Guangdong Medical College, Dongguan, PR China

ARTICLE INFO

Article history:
Received 17 February 2011
Received in revised form 29 May 2011
Accepted 23 June 2011
Available online 30 June 2011

Keywords:
Ultra-particle processing system
Microspheres
EGFP
Silk fibroin

ABSTRACT

The objective of this study was to prepare silk fibroin SF microspheres containing the enhanced green fluorescent protein (EGFP) by using a novel ultra-fine particle processing system (UPPS) and to evaluate the microspheres as possible carriers for long-term delivery of sensitive biologicals. The drug content, encapsulation efficiency, and *in vitro* release were evaluated by Microplate Absorbance Reader. The particle size distribution and morphology of the microspheres were analyzed by Malvern Master Sizer 2000 and scanning electron microscopy. The distribution of EGFP and the interactions between SF and EGFP were investigated by Confocal Laser Scanning Microscopy, FTIP, Raman and NMR spectroscopy. The results showed that spherical microspheres with narrow size distribution, glossy and dense surface were successfully manufactured by using UPPS technology and over 95% of EGFP encapsulation efficiency and uniform drug distribution in the microspheres were achieved. Furthermore, a burst free and sustained release of encapsulated EGFP for a period of 50 days in deionized water was obtained. In conclusion, the novel UPPS technology could be used to manufacture SF matrix microspheres as a potential long-term protein delivery system to improve patient compliance and convenience.

1. Introduction

Long-term protein delivery system, which contains biocompatible and biodegradable carriers to protect the therapeutic from degradation or denaturation and to control release profile, has been studied widely to improve patient compliance (Freiberg and Zhu, 2004; Ye et al., 2010). Up to now, the suitable carrier matrix and the practicable industrial preparation method are still two crucial challenges.

Silk fibroin (SF) is a structural protein that comprises silk fibers derived from cocoons which are produced by the domestic silkworm *Bombyx mori* (Wang et al., 2007). Previous research showed that SF did not cause immune response in practical applications (Meinel et al., 2005), and it could undergo proteolytic degradation and be absorbed over a long period *in vivo* (Altman et al., 2003; Horan et al., 2005; Prasong Srihanam, 2009). The important advantages of SF in the formulation of delivery systems for sensitive biologics such as therapeutic proteins and peptides are its aqueous solubility and processability under very mild conditions (Hofmann et al., 2006; Uebersax et al., 2007, 2008). For instance, SF could be recrystallized and its secondary structure could change to beta-sheet conformation by simply exposing the microspheres to an atmosphere with 96% RH (Hino et al., 2003). Preparation of SF microspheres under very mild conditions could avoid those harsh preparation conditions such as the presence of non-aqueous solvents, water/solvent interfaces, use of cross-linking reagents for hardening, or elevated temperatures (Wang et al., 2006; Wenk et al., 2008). In addition, the protective properties of SF matrices for several proteins (Demura et al., 1992; Kikuchi et al., 1999) and the long absorbing period of SF *in vivo* are of benefit to developing long-term protein delivery system which could continuously release protein drug over 7 weeks (Horan et al., 2005). Thus, SF with impressive processability, mechanical strength, biocompatibility and biodegradability, has been intensively investigated for biomedical applications as surgical suture, wound covering material, soft contact lens, scaffold for tissue engineering, and carrier for controlled release system (Cao et al., 2007; Hofmann et al., 2007; Meinel et al., 2005; Shao and Vollrath, 2002).

In general, a practicable manufacturing technology for long-term protein delivery microspheres should meet the following main requirements. Firstly, it should achieve reasonably high encapsulation efficiency and loading capacity, and the loaded pro-

* Corresponding author at: School of Pharmaceutical Sciences, Sun Yat-sen University, Guangzhou 510006, PR China. Tel.: +86 02039943120; fax: +86 02039943117.
E-mail address: cbwu2000@yahoo.com (C. Wu).

0378-5173/$ – see front matter © 2011 Elsevier B.V. All rights reserved.
doi:10.1016/j.ijpharm.2011.06.041

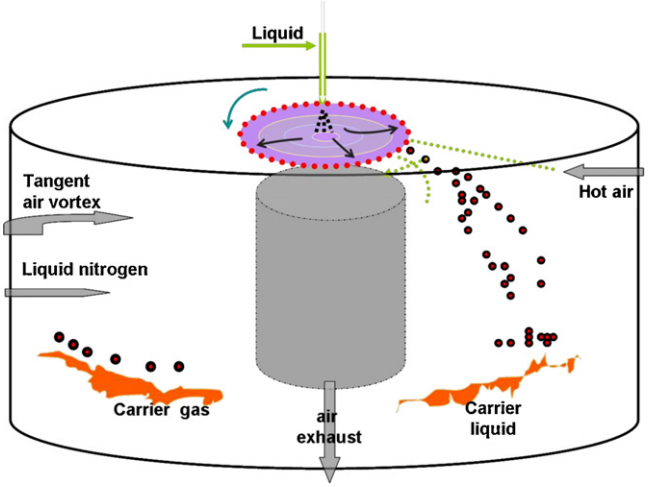

Fig. 1. Schematic illustration of UPPS equipment for manufacturing particles.

tein should retain its bioactivity and be sustainedly released (Ye et al., 2010). Secondly, the technology should demonstrate high dependability and simple operation repeatability under mild conditions to avoid detrimental effect on sensitive drugs.

A novel ultra-fine particle processing system (UPPS) was initially developed by our group, which can continuously manufacture micron-sized spherical particles with a simple and reproducible operation to control mechanical parameters. The microspheres manufactured by UPPS presented characteristics of narrow particle size distribution, glossy and dense surface, and good sphericity. The main components of UPPS include: (1) a rotating disc, (2) a feed nozzle in point shape located above the center of the rotating disc, (3) an airflow system which consists of three parts including endocentric airflow, tangent airflow, and subpressure airflow to control the movement of micro-droplets suspension, and (4) a collecting vessel with carrier gas or liquid nitrogen. The carrier gas is often the dry and cool air or nitrogen, which is controlled in process operation according to the properties of microsphere matrix. Carrier gas is necessary to further assure the particles completely dry and to move forward to the sample collector. As schematically illustrated in Fig. 1, the operating principle of UPPS can be simply described as following: a solution of drug and materials is pumped uniformly through the nozzle to the center of the high-speed rotating disc; then the liquid is compressed and sheared (Boodhoo and Jachuck, 2000; Brechtelsbauer et al., 2001; Leach et al., 2009; Tozzini et al., 2003) to a thin liquid film; subsequently, the liquid film is propelled out of the edge of the disc and forms micro-droplets. Moving with the air-flow, the micro-droplets are gradually dried to form solid microspheres. Finally, the dry microspheres are collected into the collector vessel by centrifugal forces using a high-performance cyclone.

The operating parameters of UPPS process can be precisely controlled, which include solution feeding rate, disc rotating speed, and airflow temperature, pressure and direction, etc. Therefore, this process is suitable for scale-up and industrial production, which could be applied to manufacture microspheres as drug delivery system. More importantly, UPPS has advantages in preparation of microspheres containing therapeutic proteins and peptides because of its mild operating conditions.

In this work, EGFP-silk fibroin microspheres were produced by the simple, single-step process UPPS to avoid exposing protein to harmful organic solvents. In order to develop SF matrix for the delivery of sensitive biologicals, *in vitro* evaluation and the spectroscopy investigation of the drug containing SF microspheres were carried out to study the mechanism of controlled drug release.

2. Materials and methods

2.1. Materials

Cocoons of *B. mori* were purchased from Guangxi Silk Group Co., Ltd. (Guangxi, China). Enhanced green fluorescent protein (EGFP) was kindly provided by Laboratory of Molecular Biology (School of Pharmacy of Sun Yat-sen University). All other chemicals were obtained commercially at analytical grade.

2.2. Preparation of EGFP-SF microspheres by UPPS

SF was prepared from cocoons of *B. mori* as previous reference described (Ajisawa, 1998; Bayraktar et al., 2005; Yamada et al., 2001). Briefly, cocoons were boiled in an aqueous solution of 0.02 M Na_2CO_3 for 20 min twice and thoroughly rinsed with deionized water to remove sericin (degumming). The extracted SF was then dissolved in a $CaCl_2$–ethanol–water solution (mole ratio = 1:2:8, Ajisawa's reagent) under stirring at 78 °C for 2 h. The resulting fibroin solution was centrifugally separated at 5000 rpm for 15 min, and the supernatant was dialyzed in a cellulose tube (Viskase, USA; MWCO 14 kDa) against deionized water for 3 days until the dialyzate was tested negative for chloride ion using $AgNO_3$. Finally, the dialyzated solution was freeze dried at −20 °C for 30 h (CHRiST, Germany) and cotton-like SF solid was obtained and stored in an airtight container at room temperature.

In an ice-water bath, 1 g of SF solid was dissolved in 19 ml and 10 ml of deionized water under magnetic stirring to obtain 5% and 9% (w/w) of SF solution, respectively. Then 10 mg of EGFP was dissolved in each of the SF solutions.

Under the computer control of UPPS process parameters, the EGFP-SF solution was supplied to the nozzle by a peristaltic pump (EYELA MP-1000, Japan) at a flow rate of 4.0 ml/min. The disc spinning speed was set at 9000 rpm, the pressure and temperature of endocentric airflow and tangent airflow were set at 15 psi and 35 °C, 10 psi and 25 °C, respectively, and the pressure of subpressure airflow was set at 5 psi. These parameters were chosen on the basis of pilot experiments which produced acceptable solid particles repeatedly. Nevertheless, a number of experiments were also performed at different disc spinning speeds and EGFP-SF solution concentrations to establish a proof-of-principle.

The product of SF microspheres was vacuum dried at 0.18 mbar and room temperature for 2 h (CHRiST, Germany) to remove any residual water.

For water vapor treatment, the dried microspheres were exposed to water vapor of 96% relative humidity in the presence of a saturated aqueous solution of Na_2SO_4 at room temperature for 24 h as previously described (Hino et al., 2003).

2.3. Characterization of EGFP-SF microspheres

2.3.1. Particle size analysis

The particle size determination of microsphere was conducted using a dry method mode of Malvern Master Sizer 2000 (Malvern Instruments, UK). The particle size was determined by measuring the diameter of spheres in the same sample volume and dispersing the particles with a 2 bar compressed air stream.

2.3.2. Confocal laser scanning microscopy (CLSM)

The distribution of EGFP inside the SF microspheres was analyzed on the basis of microscopic images taken by a confocal laser scanning microscopy ZEISS LSM 710 (Carl Zeiss, Germany). Dry powdery samples of microspheres were sown on glass slides and photographed. The excitation wavelength was selected as 488 nm.

2.3.3. Scanning electron microscopy (SEM)

To image the interior structure of the EGFP-SF microspheres, dry microspheres were fractured by a razor blade to show their cross-sections. Intact or fractured microspheres were placed on metal sample holders and gold coated using a gold sputter module in a high vacuum evaporator. Coated samples were then examined by SEM (JSM-6330F, JEOL Ltd., Japan) at 15 kV.

2.3.4. Fourier-transform infrared spectroscopy (FTIR)

EGFP-SF microspheres or comparing samples were mixed with KBr and compressed to KBr disks for FTIR spectroscopy examination performed on a Bruker Tensor 37 spectrophotometer (Bruker, Germany). All the spectra were recorded in the range of 400–4000 cm^{-1}. The spectrum of each sample was acquired by accumulating 32 scans with a resolution of 4 cm^{-1}.

2.3.5. Laser micro-Raman spectroscopy

Raman microscope analyses were performed in order to understand the interactions between EGFP and SF, which may affect the long-term release of EGFP from the microspheres. Dry EGFP-SF microspheres were sown on glass slides and analyzed with Raman microscopic (Renishaw Invia Raman Microscope, UK). The raw spectra were not smoothed and the baseline features of fluorescence intensity of the samples were remained.

2.3.6. Hydrogen nuclear magnetic resonance (HNMR) spectroscopy

HNMR analysis was performed on EGFP-SF microspheres to check any structure changes of EGFP and SF in the microspheres. At least 10 mg of microspheres was placed into glass NMR sample tube with 0.5 ml of Deuterium Oxide (Cambridge Isotope Laboratories, Inc., USA). The proton NMR spectra were acquired on a NMR spectrometer (Bruker Ultrashield 400 Plus, Germany) operating at 400 MHz and 25 °C. All data were processed using MestReNova software.

2.4. Drug content and encapsulation efficiency

The actual content of model drug EGFP in the SF microspheres was determined by dissolving 5 mg of untreated microspheres in 1 ml of deionized water. The concentration of EGFP was analyzed by measuring absorbance with the excitation and emission of fluorescence at 488 nm and 510 nm, respectively, using a Multimode Microplate Reader (Infinite M1000, Tecan, Switzerland). No drug leakage from SF microspheres was expected to occur upon exposing to water vapor. Therefore, the actual drug content was assumed identical in both water vapor treated and untreated SF microspheres.

Theoretical drug content was calculated by assuming the entire amount of drug added to the SF solution was encapsulated and no drug loss occurred at any stage of SF microsphere preparation. Encapsulation efficiency was calculated as the percentage of actual versus theoretical drug content.

2.5. In vitro drug release

The study of EGFP release from SF microspheres was conducted by incubating 5 mg of microsphere sample in 5 ml of deionized water at 25 °C for 55 days. Previously it was found that the fluorescence invariableness of EGFP aqueous solution could be preserved at this temperature for at least 7 days. The release medium was fully replaced with fresh medium after 1, 2, 4, 8, 12 h, and 1, 2, 3, 5, 7, 10, 14, 21, 28, 35, 42, 50, and 55 days. At each sampling time point, 200 μl of release medium was pipetted to each well of a black 96-well plate for detection of fluorescence assay using a Microplate Absorbance Reader with excitation and emission of fluorescence at 488 nm and 510 nm, respectively.

The fluorescence absorbance of solution without EGFP (negative control) was defined as 0. Additionally, absorbance of standard solutions containing 0.1, 0.5, 1.0, 5.0 and 10.0 μg/ml of EGFP (positive controls) was measured to assure the range of linear relationship between absorbance and EGFP concentration.

3. Results and discussion

3.1. Characterization of EGFP-SF microspheres

3.1.1. Particle size analysis

In the preparation of microspheres using UPPS, 9% of SF solution was processed into SF microspheres at varying disc rotating speed of 6000, 9000, and 12,000 rpm, respectively. The mean volume diameters of microspheres prepared with 9% SF solution at 6000, 9000, 12,000 rpm, and 5% SF solution at 9000 rpm were 63.2, 42.3, 29.8, and 38.3 μm, respectively, as shown in Fig. 2. These results indicated the microspheres had narrow size distribution. Though the size distribution was not apparently affected by the rotating speed of UPPS disc, it was found microspheres with smaller mean size were produced at higher rotating speed.

At a set disc rotating speed of 9000 rpm, the particle size of microspheres was also affected by the concentration of SF solution. When the concentration of SF solution was decreased from 9% to 5%, the produced microspheres showed slightly larger mean size and wider size distribution, which could be ascribed to the smaller liquid droplet formed during spinning process and slower solidification led to more chance merging droplets together with the lower concentration SF solution.

3.1.2. Microscopic properties

Microspheres produced at disc rotating speed of 9000 rpm from 5% and 9% SF solutions, which were simply denoted as 5% and 9% microspheres, were examined for surface morphology.

SEM micrographs in Fig. 3A and C revealed that the SF microspheres were typically in spherical shape, but the sags on the dense surface leaving the microspheres a dry jujube-like surface. Formation of this surface could be explained as following: in the processing of microspheres, SF micro-droplets moved with the airflow to gradually dry and form solid microspheres relatively slowly. It could be speculated that as the solvent evaporated, the micro-droplet could be encapsulated by a layer of thin film formed by

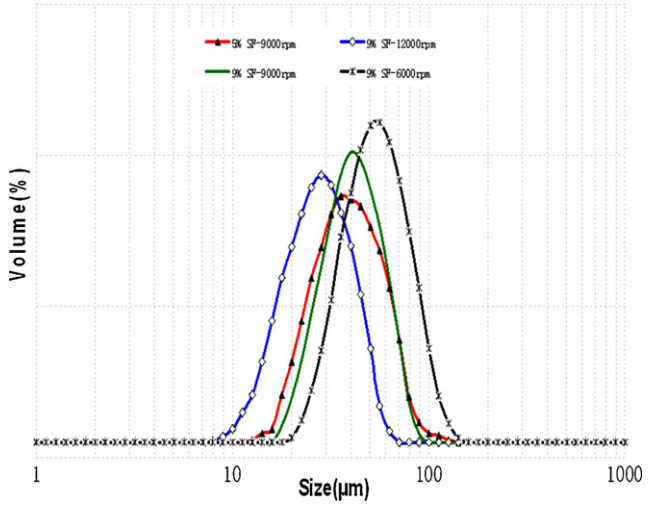

Fig. 2. Influence of UPPS disc rotating speed and SF concentration on the size distribution of SF microspheres.

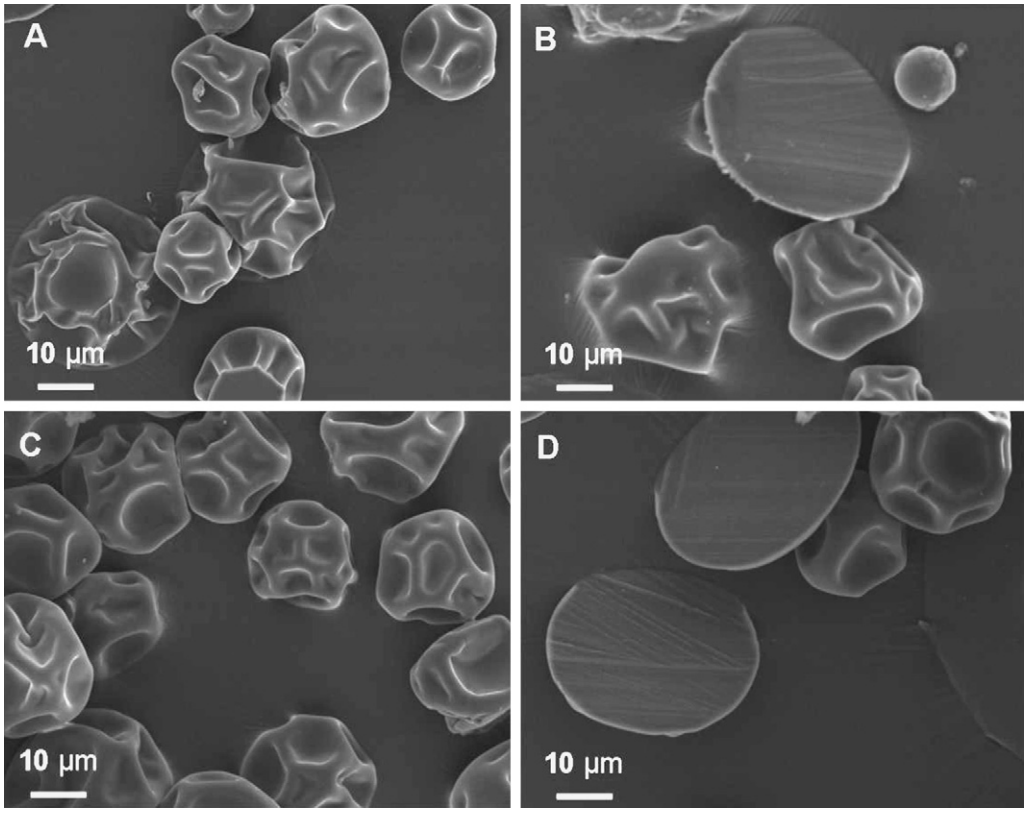

Fig. 3. SEM micrographs of EGFP-SF microspheres, (A) 5% SF; (B) cross-section of 5% SF; (C) 9% SF; and (D) cross-section of 9% SF.

the material which was continuously separated from the SF solution. Then the evaporation of the inner solvent would cause the droplets to contract inward and the outside thin film was not strong enough to withstand this retraction strength, hence the relatively weak parts of the film would sink to form sags and leave a dry jujube-like surface.

The cross-section micrographs of SF microspheres in Fig. 3B and D showed that the internal parts of the microspheres were dense, and there was not apparent difference between 9% and 5% SF micospheres.

3.2. Encapsulation efficiency and drug distribution in microspheres

The encapsulation efficiency of 5% and 9% microspheres calculated from EGFP assay was 98.8 ± 0.95 and 99.5 ± 1.25, respectively. Actually, a high encapsulation efficiency of 95% above was consistently achieved by UPPS and it was not related to the carrier material and drug (microspheres with other model drugs and carrier materials were prepared using UPPS and the high encapsulation efficiency data were not shown here). This is because the non-volatile drugs have no chance to leak during the preparation of microspheres in UPPS.

The distribution of EGFP in 9% microspheres was analyzed using CLSM, and the micrographs under fluorescence and nature lights were shown in Fig. 4. By merging the graph of EGFP displayed under fluorescence (Fig. 4A) with the image of EGFP-SF microspheres under natural light (Fig. 4B), a uniform distribution of EGFP in the matrix of SF microspheres was revealed (Fig. 4C).

3.3. In vitro drug release

The cumulative release profiles of EGFP in deionized water from 5% and 9% microspheres which were water vapor treated under 96% RH for 24 h to gain the property of sustained-release of bioactive agents from SF matrix are shown in Fig. 5 (Wenk et al., 2008). The 9%

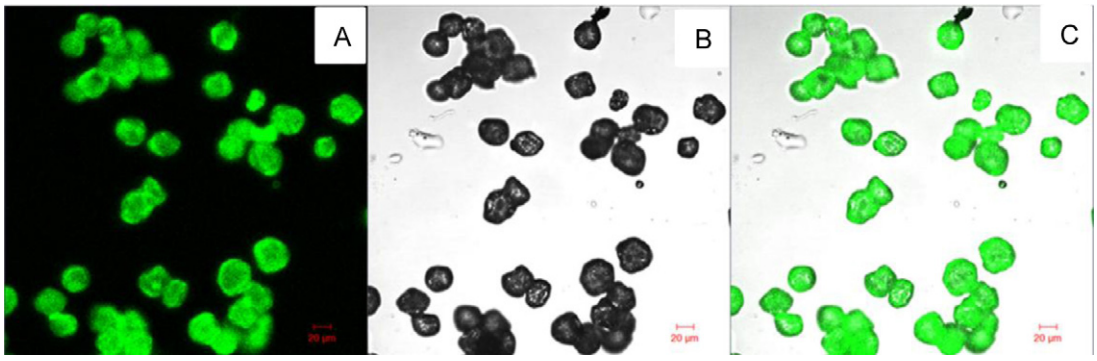

Fig. 4. CLSM micrographs of EGFP-SF microspheres under different lights, (A) fluorescence; (B) natural light; and (C) mergence of (A) and (B).

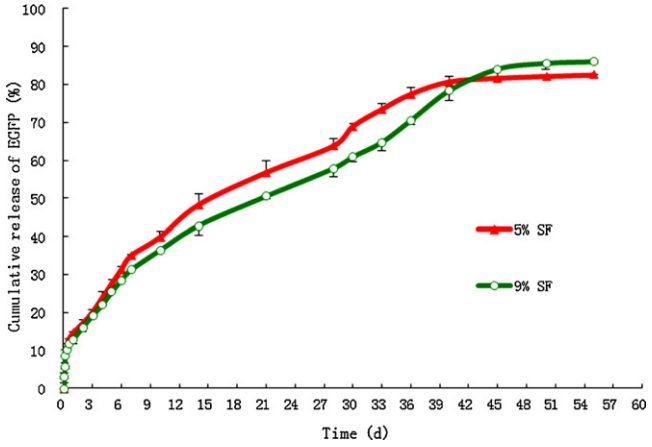

Fig. 5. Release profiles of EGFP in deionized water from EGFP-SF microspheres after water vapor treated under 96% RH for 24 h ($n = 5$).

microspheres showed an initial release of 3.2 wt% in the first hour and 13.0 wt% release in the first day. Overall, 85 wt% of encapsulated EGFP was released from 9% microspheres over a period of 50 days. For 5% microspheres with less SF, 3.5 wt% of EGFP was released in the first hour, 14.7 wt% was released in the first day, and a total of 82 wt% was released in 50 days. Clearly, a long-term release of EGFP from the SF matrix was obtained.

No obvious burst release in the first hour was shown in EGFP release profiles which further confirmed that the drug was indeed encapsulated and distributed inside the SF microspheres through the UPPS preparation process, rather than attached on the surface of microspheres.

3.4. FTIR, Raman, and HNMR spectroscopies of SF microspheres

It was observed that SF material and SF microspheres produced by UPPS dissolved in water quickly, while water vapor treated SF microspheres could suspend in water to achieve a long-term release of EGFP. This suggested that some changes occurred in the EGFP-SF microspheres during the vapor treatment which induced a sustained release mechanism. FTIR, Raman, and HNMR spectroscopies were employed to investigate the interactions between encapsulated EGFP and SF matrix in the microspheres. The spectra of EGFP-SF microspheres prepared from 9% SF solutions were recorded and shown in Fig. 6 to compare with the spectra of SF and EGFP materials.

As shown in Fig. 6A, the FTIR spectra of SF material and SF microspheres in the region of 3000 to 3600 cm^{-1} all presented bands at 3300 cm^{-1} and 3200 cm^{-1} which were due to the hydrogen-bonded N–H and O–H stretching vibration, respectively. For SF material, the strong band at 3260 cm^{-1} with an extending shoulder at 3500 cm^{-1} suggested that there was intra- or inter-molecular hydrogen bond formed in SF. For untreated EGFP-SF microspheres, the corresponding band was greatly broadened and slightly shifted to high frequency to form a very wide band ranged from 3200 to 3500 cm^{-1}. This indicated that a new hydrogen bond was formed in EGFP-SF microsphere due to the interactions between EGFP and SF. As comparing to the spectrum of vapor treated EGFP-SF microspheres, the band shifted more and became narrower with a range from 3385 to 3450 cm^{-1}. This may be related to the reconstruction of hydrogen bond caused by the conformation change of EGFP and SF molecules in vapor treated microsphere (Gao et al., 2000).

It was reported previously that the characteristic peaks at 1660, 1545, and 1230 cm^{-1} in SF spectrum were corresponding to the random coil/or α-helix structure of amide I, amide II, amide III regions, respectively. And these bands would shift to 1630, 1520, and 1260 cm^{-1} for SF with β-sheet structure.

For amide I region (mainly attributed to the C=O stretching vibration), the single band at 1655 cm^{-1} in SF spectrum showed that there was mainly random coil structure in SF material. In spectrum of EGFP-SF microspheres, the broad band ranged from 1700 to 1640 cm^{-1} suggested that the structure of SF was changed and the 1700 cm^{-1} band was an evidence for C=O partially involving the formation of hydrogen bond. The spectrum of vapor treated microspheres showed the band shifted to 1625 cm^{-1} and it implied the random coil conformation of SF transited to β-sheet conformation.

For amide II region, SF spectrum showed a single-peak at 1545 cm^{-1}. In spectrum of untreated EGFP-SF microspheres, the band shifted to 1520 cm^{-1} leaving a shoulder at 1545 cm^{-1}, which suggested there was β-sheet conformation of SF in microspheres. In spectrum of vapor treated microspheres, the 1545 cm^{-1} band shifted to 1550 cm^{-1} with increased intensity and the 1520 cm^{-1} band remained with weakened intensity, and this revealed the effect of EGFP and SF interaction on β-sheet conformation of SF.

For amide III region with one band appearing at 1230 cm^{-1}, there was no obvious difference between spectra of SF material and microspheres. However, in the spectrum of vapor treated microspheres this band was weakened and shifted to 1260 cm^{-1}, where the characteristic band of β-sheet conformation typically exists.

Overall, the comparison of FTIR spectra in Fig. 6A demonstrated that the hydrogen-bonding interaction between SF and EGFP in microspheres caused the conformation change of SF molecules, and this effect was more noticeably on N–H stretching vibration, amide I and amide II regions. The structure of SF in EGFP-SF microspheres was mainly random coil conformation, while the structure of SF in vapor treated microspheres was transformed to β-sheet conformation. This was consistent with the water solubility of random coil and β-sheet conformation of SF. The results also suggested the process of UPPS was moderate and did not significantly impact the conformation of SF during the microsphere preparation (Litvinenko and Meech, 2004; Monti et al., 2007).

The Raman spectrum (Fig. 6B) of untreated EGFP-SF microspheres showed amide I bands at 1660 cm^{-1}, amide III bands at 1251, and ν_{cc} skeletal stretching band at 1102 cm^{-1}. All these bands were attributed to α-helix and/or random coil conformation of SF (Hino et al., 2003; Lefevre et al., 2007; Zheng et al., 2010). For vapor treated EGFP-SF microspheres, the characteristic bands appeared near 1667 cm^{-1} (amide I), 1232 cm^{-1} (amide III), and 1085 cm^{-1} (ν_{cc} skeletal stretching), respectively, which represented the characteristic bands of β-sheet structure of SF (Monti et al., 2001; Tozzini et al., 2003). The Raman spectroscopy results further confirmed that the molecular conformation of SF in matrix microspheres obviously changed from random coil conformation to β-sheet structure during vapor treatment.

By comparing the HNMR spectra of SF, EGFP, vapor treated and untreated EGFP-SF microspheres in Fig. 6C, it was observed the chemical shifts of SF β-sheet structure at 6.7 and 7.0 ppm (N–H) and the chemical shift of EGFP at 1.8 ppm (β–H) all disappeared in the spectrum of vapor treated EGFP-SF microspheres (Ashida et al., 2002; Hori et al., 2001; Kameda et al., 2003; McLachlan et al., 2009; Jackson et al., 2006; Zhao and Asakura, 2001). Although it was not clear what specific effects occurred in vapor treated EGFP-SF microspheres, it could be speculated that the hydrogen bonding formed between SF and EGFP molecules might impact the HNMR spectra.

Moreover, the characteristic absorption bands of FTIR and Raman were not significantly different between untreated EGFP-SF microspheres and SF material, as main features of α-helix and/or random coil conformation were presented. This indicated UPPS is a relatively mild processing technology for preparation of microspheres and it is benefit to the stability of sensitive drugs. Previous

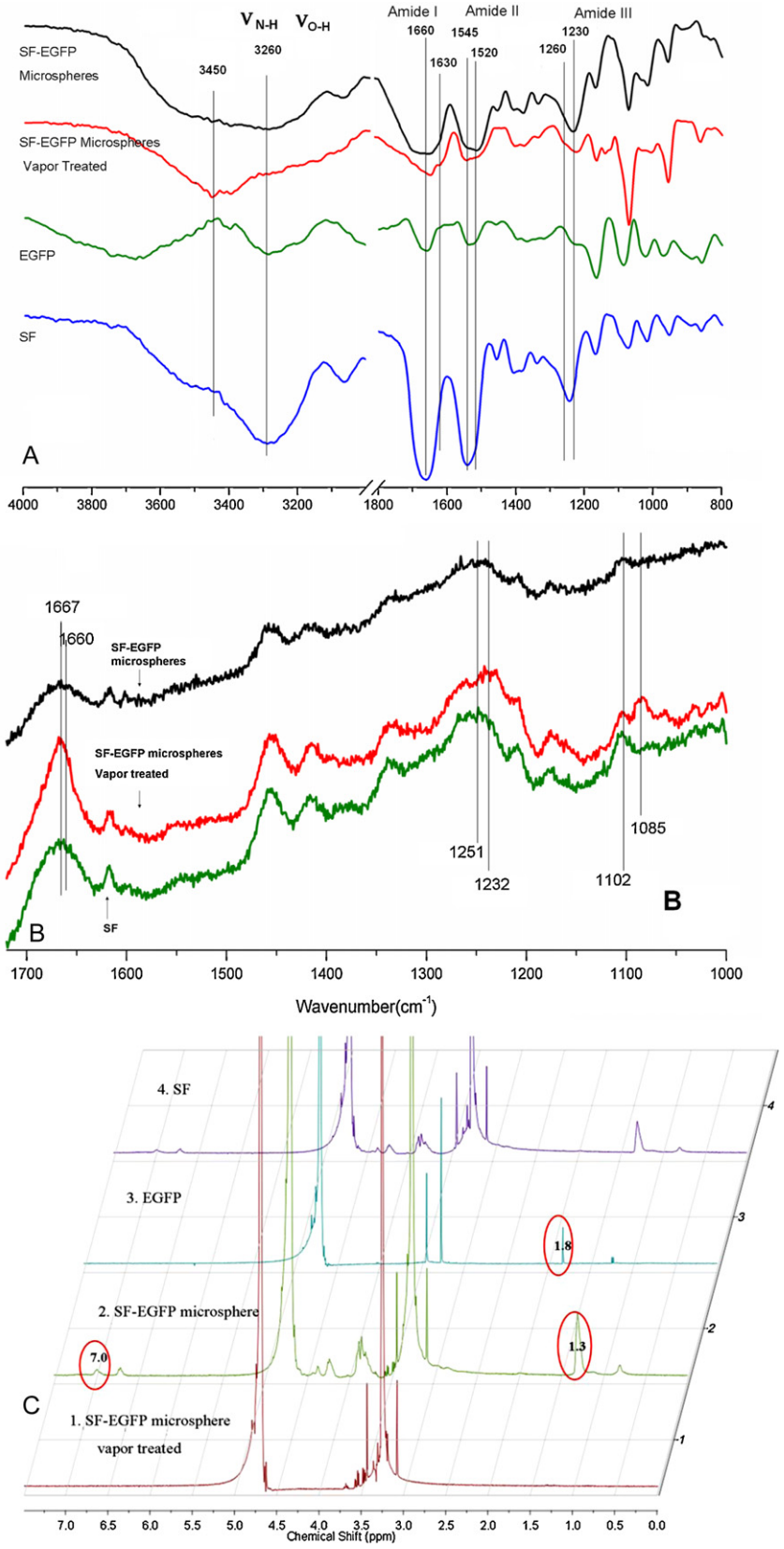

Fig. 6. Comparison of spectra to show the interactions between EGFP and SF matrix in microspheres. (A) FTIR; (B) Raman spectroscopy; and (C) HNMR.

documents demonstrated that silk fibroin has excellent properties such as biocompatibility, biodegradation, non-toxicity, adsorption properties and that the silk-based biomaterials including β-sheet conformation SF was susceptible to proteolytic degradation *in vivo* and over longer periods it would be absorbed (Cao and Wang, 2009; Wang et al., 2008). There was not obvious difference in β-sheet conformation SF between the SF microspheres after treated at 96%RH and treated SF material reported in the literatures (Wang et al.,

2008). Therefore the SF microspheres after treated at 96% RH could have similar biodegradability to the silk fibroin.

It was observed in a separate study that the peptide with higher molecular weight achieved a longer term of release from SF matrix microspheres (data were not shown). Thus, it can be speculated that van der Waals force might play an important role in the interactions between SF and protein. The joint interactions of hydrogen bonds and van der Waals force between EGFP and SF may be the main mechanisms for sustained release of EGFP from SF matrix.

4. Conclusions

The current study demonstrated that microspheres manufactured with UPPS presented many advantageous characteristics such as narrow particle size distribution, glossy and dense surface, satisfying sphericity, and uniform drug distribution in matrix. Through controlling of the processing parameters, UPPS was proved to be a single-step simple process and encapsulation efficiency suitable for scale-up to industrial production. Comparing to the emulsifying microsphere preparation methods, UPPS could provide a useful new idea to bypass the common problems such as the use of potential toxic surfactants and cross-linking agents, low encapsulation efficiency, no the water-washed step for removing residual agents in preparation of microsphere. More importantly, the mild UPPS operation conditions are of benefit to protecting the encapsulated proteins and peptides in SF matrix. The prepared microspheres could be use as a carrier for sustained-release injections due to the biocompatibility and biodegradation of SF and long-term release of therapeutic proteins and peptides from SF matrix. However, UPPS method may be limited by material properties of viscosity and solubility, because it is difficult to manufacture microspheres from too sticky material. Some materials need special studies to identify the proper range of concentration for UPPS processing.

Acknowledgements

The authors are grateful to professor Du Jun, Laboratory of Molecular Biology, School of Pharmacy of Sun Yat-sen University, for generous gift samples of EGFP. The work was supported by National Science and Technology Foundation of China "The Creation for Significant New Drugs" (2009ZX09501-023) and major projects of Science and Technology Foundation of Guangzhou (2008A1-E4101-1).

References

Ajisawa, A., 1998. Dissolution of silk fibroin with calcium chloride–ethanol aqueous solution. J. Seric. Sci. Jpn. 67, 91–94.
Altman, G.H., Diaz, F., Jakuba, C., Calabro, T., Horan, R.L., Chen, J.S., Lu, H., Richmond, J., Kaplan, D.L., 2003. Silk-based biomaterials. Biomaterials 24, 401–416.
Ashida, J., Ohgo, K., Asakura, T., 2002. Determination of the torsion angles of alanine and glycine residues of *Bombyx mori* silk fibroin and the model peptides in the silk I and silk II forms using 2D spin diffusion solid-state NMR under off magic angle spinning. J. Phys. Chem. B 106, 9434–9439.
Bayraktar, O., Malay, O., Ozgarip, Y., Batigun, A., 2005. Silk fibroin as a novel coating material for controlled release of theophylline. Eur. J. Pharm. Biopharm. 60, 373–381.
Boodhoo, K.V.K., Jachuck, R.J., 2000. Process intensification: spinning disk reactor for styrene polymerisation. Appl. Therm. Eng. 20, 1127–1146.
Brechtelsbauer, C., Lewis, N., Oxley, P., Ricard, F., Ramshaw, C., 2001. Evaluation of a spinning disc reactor for continuous processing. Org. Process Res. Dev. 5, 65–68.
Cao, Y., Wang, B.C., 2009. Biodegradation of silk biomaterials. Int. J. Mol. Sci. 10, 1514–1524.
Cao, Z.B., Chen, X., Yao, J.R., Huang, L., Shao, Z.Z., 2007. The preparation of regenerated silk fibroin microspheres. Soft Matter 3, 910–915.
Demura, M., Takekawa, T., Asakura, T., Nishikawa, A., 1992. Characterization of low-temperature-plasma treated silk fibroin fabrics by ESCA and the use of the fabrics as an enzyme-immobilization support. Biomaterials 13, 276.
Freiberg, S., Zhu, X., 2004. Polymer microspheres for controlled drug release. Int. J. Pharm. 282, 1–18.
Gao, Q.W., Shao, Z.Z., Sun, Y.Y., Lin, H., Zhou, P., Yu, T.Y., 2000. Complex formation of silk fibroin with poly(acrylic acid). Polym. J. 32, 269–274.
Hino, T., Tanimoto, M., Shimabayashi, S., 2003. Change in secondary structure of silk fibroin during preparation of its microspheres by spray-drying and exposure to humid atmosphere. J. Colloid Interface Sci. 266, 68–73.
Hofmann, S., Foo, C., Rossetti, F., Textor, M., Vunjak-Novakovic, G., Kaplan, D.L., Merkle, H.P., Meinel, L., 2006. Silk fibroin as an organic polymer for controlled drug delivery. J. Control. Release 111, 219–227.
Hofmann, S., Hagenmuller, H., Koch, A.M., Muller, R., Vunjak-Novakovic, G., Kaplan, D.L., Merkle, H.P., Meinel, L., 2007. Control of in vitro tissue-engineered bone-like structures using human mesenchymal stem cells and porous silk scaffolds. Biomaterials 28, 1152–1162.
Horan, R.L., Antle, K., Collette, A.L., Huang, Y.Z., Huang, J., Moreau, J.E., Volloch, V., Kaplan, D.L., Altman, G.H., 2005. In vitro degradation of silk fibroin. Biomaterials 26, 3385–3393.
Hori, Y., Demura, M., Iwadate, M., Ulrich, A.S., Niidome, T., Aoyagi, H., Asakura, T., 2001. Interaction of mastoparan with membranes studied by H-1-NMR spectroscopy in detergent micelles and by solid-state H-2-NMR and N-15-NMR spectroscopy in oriented lipid bilayers. Eur. J. Biochem. 268, 302–309.
Jackson, S.E., Craggs, T.D., Huang, J.-r., 2006. Understanding the folding of GFP using biophysical techniques. Expert Rev. Proteomics 3, 545–559.
Kameda, T., Zhao, C.H., Ashida, J., Asakura, T., 2003. Determination of distance of intra-molecular hydrogen bonding in (Ala-Gly)(15) with silk I form after removal of the effect of MAS frequency in REDOR experiment. J. Magn. Reson. 160, 91–96.
Kikuchi, J., Mitsui, Y., Asakura, T., Hasuda, K., Araki, H., Owaku, K., 1999. Spectroscopic investigation of tertiary fold of staphylococcal protein A to explore its engineering application. Biomaterials 20, 647–654.
Leach, J., Mushfique, H., Keen, S., Di Leonardo, R., Ruocco, G., Cooper, J.M., Padgett, M.J., 2009. Comparison of Faxen's correction for a microsphere translating or rotating near a surface. Phys. Rev. E, 79.
Lefevre, T., Rousseau, M.E., Pezolet, M., 2007. Protein secondary structure and orientation in silk as revealed by Raman spectromicroscopy. Biophys. J. 92, 2885–2895.
Litvinenko, K.L., Meech, S.R., 2004. Observation of low frequency vibrational modes in a mutant of the green fluorescent protein. Phys. Chem. Chem. Phys. 6, 2012–2014.
McLachlan, G.D., Slocik, J., Mantz, R., Kaplan, D., Cahill, S., Girvin, M., Greenbaum, S., 2009. High-resolution NMR characterization of a spider-silk mimetic composed of 15 tandem repeats and a CRGD motif. Protein Sci. 18, 206–216.
Meinel, L., Hofmann, S., Karageorgiou, V., Kirker-Head, C., McCool, J., Gronowicz, G., Zichner, L., Langer, R., Vunjak-Novakovic, G., Kaplan, D.L., 2005. The inflammatory responses to silk films in vitro and in vivo. Biomaterials 26, 147–155.
Monti, P., Freddi, G., Arosio, C., Tsukada, M., Arai, T., Taddei, P., 2007. Vibrational spectroscopic study of sulphated silk proteins. J. Mol. Struct. 834, 202–206.
Monti, P., Taddei, P., Freddi, G., Asakura, T., Tsukada, M., 2001. Raman spectroscopic characterization of *Bombyx mori* silk fibroin: Raman spectrum of Silk I. J. Raman Spectrosc. 32, 103–107.
Prasong Srihanam, W.S., 2009. Proteolytic degradation of silk fibroin scaffold by protease XXIII. Open Macromol. J. 3, 1–5.
Shao, Z.Z., Vollrath, F., 2002. Materials: surprising strength of silkworm silk. Nature 418, 741–1741.
Tozzini, V., Bizzarri, A.R., Pellegrini, V., Nifosi, R., Giannozzi, P., Iuliano, A., Cannistraro, S., Beltram, F., 2003. The low frequency vibrational modes of green fluorescent proteins. Chem. Phys. 287, 33–42.
Uebersax, L., Mattotti, M., Papaloizos, M., Merkle, H.P., Gander, B., Meinel, L., 2007. Silk fibroin matrices for the controlled release of nerve growth factor (NGF). Biomaterials 28, 4449–4460.
Uebersax, L., Merkle, H.P., Meinel, L., 2008. Insulin-like growth factor I releasing silk fibroin scaffolds induce chondrogenic differentiation of human mesenchymal stem cells. J. Control. Release 127, 12–21.
Wang, L.Y., Gu, Y.H., Su, Z.G., Ma, G.H., 2006. Preparation and improvement of release behavior of chitosan microspheres containing insulin. Int. J. Pharm. 311, 187–195.
Wang, X.Q., Wenk, E., Matsumoto, A., Meinel, L., Li, C.M., Kaplan, D.L., 2007. Silk microspheres for encapsulation and controlled release. J. Control. Release 117, 360–370.
Wang, Y., Rudym, D.D., Walsh, A., Abrahamsen, L., Kim, H.J., Kim, H.S., Kirker-Head, C., Kaplan, D.L., 2008. In vivo degradation of three-dimensional silk fibroin scaffolds. Biomaterials 29, 3415–3428.
Wenk, E., Wandrey, A., Merkle, H., Meinel, L., 2008. Silk fibroin spheres as a platform for controlled drug delivery. J. Control. Release 132, 26–34.
Yamada, H., Nakao, H., Takasu, Y., Tsubouchi, K., 2001. Preparation of undegraded native molecular fibroin solution from silkworm cocoons. Mater. Sci. Eng. C 14, 41–46.
Ye, M., Kim, S., Park, K., 2010. Issues in long-term protein delivery using biodegradable microparticles. J. Control. Release.
Zhao, C.H., Asakura, T., 2001. Structure of silk studied with NMR. Prog. Nucl. Magn. Reson. Spectrosc. 39, 301–352.
Zheng, Z.H., Wei, Y.Q., Yan, S.Q., Li, M.Z., 2010. Preparation of regenerated *Antheraea yamamai* silk fibroin film and controlled-molecular conformation changes by aqueous ethanol treatment. J. Appl. Polym. Sci. 116, 461–467.